Journal of ELECTRONIC MATERIALS, Vol. 49, No. 8, 2020
https://doi.org/10.1007/s11664-020-08266-9

TOPICAL COLLECTION: 19TH INTERNATIONAL CONFERENCE ON II-VI COMPOUNDS

The Properties of $Cd_{1-x}Zn_xTe$ Films Prepared by RF Magnetron Sputtering

TONGYING WANG,[1] JIAN HUANG,[1,2] ZHUORUI CHEN,[1] HAOFEI HUANG,[1] HONGWEI LI,[1] KE TANG,[1] MENG CAO,[1] and LINJUN WANG[1,3]

1.—School of Materials Science and Engineering, Shanghai University, Shanghai 200444, P.R. China. 2.—e-mail: jianhuang@shu.edu.cn. 3.—e-mail: ljwang@shu.edu.cn

$Cd_{1-x}Zn_xTe$ films were prepared on borosilicate glass substrate using RF magnetron sputtering in this work. The effects of sputtering power, sputtering pressure and substrate temperature on the properties of the films were investigated in detail. The films were annealed in $CdCl_2$ atmosphere for 2 h at 200 °C, 300 °C, and 400 °C, respectively. The effects of annealing treatment on the properties of the films were also investigated. The properties of the films were investigated by x-ray diffraction, atomic force microscopy, and current–voltage (*I–V*) characterization. The results indicate that crystalline quality and the average grain size of the films increases with the increases of sputtering power. The grain size of the films becomes larger as the substrate temperature increases. The Zn concentration of the films rises as the sputtering pressure increases. After annealing, the grain size of the films becomes larger, furthermore, the resistivity decreases.

Key words: $Cd_{1-x}zn_xte$ films, RF magnetron sputtering, annealing

INTRODUCTION

$Cd_{1-x}Zn_xTe$, an II–VI Group compound semiconductor with zinc blende structure, is widely used in room temperature nuclear radiation detectors, solar cells,[1] light emitting diodes,[2] photoconductors[3] and other fields due to its high resistivity, large atomic number (about 43) and excellent carrier characteristics.[4] It is well known that the performance of single crystal materials are better than those of polycrystalline films, but it is not easy to prepare high quality large area single crystal, which limits the application of single crystal materials.[5] Therefore, $Cd_{1-x}Zn_xTe$ polycrystalline films are popular among researchers because of their rapid and large-area preparation.

There are many methods to prepare $Cd_{1-x}Zn_xTe$ films, such as closed-space sublimation (CSS),[6] electron beam evaporation,[7] pulsed laser deposition,[8] chemical bath deposition,[9] molecular beam epitaxy,[10] and RF magnetron sputtering.[11] The preparation of $Cd_{1-x}Zn_xTe$ films by RF magnetron sputtering is characterized by good uniformity and ease of control.[12]

Annealing is a common process for film post-treatment to improve the properties of films.[6,13,14] So far, only a few results have reported about the preparation and annealing of $Cd_{1-x}Zn_xTe$ films by magnetron sputtering.[15,16] The effects of sputtering parameters and post-annealing treatment on the properties of $Cd_{1-x}Zn_xTe$ films have not been studied systematically. In this work, the $Cd_{1-x}Zn_xTe$ films were prepared by RF magnetron sputtering. The influence of the deposition parameters of magnetron sputtering (sputtering power, sputtering pressure, substrate temperature) and $CdCl_2$ atmosphere annealing on the structure, surface morphology and electrical properties of $Cd_{1-x}Zn_xTe$ films were studied in detail.

(Received December 3, 2019; accepted June 9, 2020; published online June 24, 2020)

EXPERIMENTAL DETAILS

$Cd_{1-x}Zn_xTe$ films were deposited on borosilicate glass substrate ($19.5 \times 19.5 \times 0.7$ mm^3) by RF magnetron sputtering. A 50-mm diameter $Cd_{0.8}Zn_{0.2}Te$ (99.99%) target was used during the deposition process. Base pressure before sputtering was 6.0×10^{-4} Pa and high purity Ar (99.999%) gas was used in sputtering process. The distance between the target and the substrate is 6 cm. Substrates were first cleaned ultrasonically with acetone, methanol and deionized water for 10 min and dried with nitrogen. The thicknesses of all the prepared films were about 500 nm controlled by a vibrating quartz crystal. The influence of sputtering power, sputtering pressure and substrate temperature on the properties of $Cd_{1-x}Zn_xTe$ films was investigated. Detailed deposition parameters were shown in Table I. After deposition, the prepared $Cd_{1-x}Zn_xTe$ films were coated with $CdCl_2$ ethanol solution with a spin coater followed by annealing under vacuum with the temperature range of 200–400 °C for 2 h.

The structure of the $Cd_{1-x}Zn_xTe$ films was evaluated by x-ray diffraction (XRD, D/MAX–2200 V PC 3 kW, CuKα1, λ = 0.15406 nm). The surface morphology of $Cd_{1-x}Zn_xTe$ films samples were characterized by atomic force microscopy (AFM). GZO (Ga doped-ZnO) electrodes with thickness of about 120 nm were deposited on $Cd_{1-x}Zn_xTe$ film by RF magnetron sputtering and the current–voltage (I–V) characteristics were measured using a Keithley 4200/SCS digital semiconductor characterization system.

RESULTS AND DISCUSSION

XRD patterns of CdZnTe films deposited at different sputtering powers from 50 W to 125 W are shown in Fig. 1. The results indicate that all the films showed (111) preferred orientation with a zinc blend structure (JCPDS 53–0552/0553).[17] The intensity of the (111) diffraction peak increases and the full width at half maximum (FWHM) of the (111) peak decreases as the sputtering power increases. A better crystalline quality was obtained for the films grown at 125 W with the smaller FWHM value.[18]

The grain size of the films was also calculated by Scherrer's formula equation.[19,20]

$$D(hkl) = \frac{k\lambda}{\beta \cos\theta} \quad (1)$$

where β is the FWHM of (111) peak, k = 0.89, λ (1.5418 Å) is the wavelength of radiation used in XRD characterization, and θ is the Bragg angle at peak position. The calculated results are shown in Table II. With the increase of sputtering power, the grain size of the film increases gradually.

Figure 2 shows the AFM images of the films which can be found that the grain size of the film increases with the increasing of sputtering power. This is consistent with the XRD results. The results also show that all the films are very smooth with small value of surface roughness.

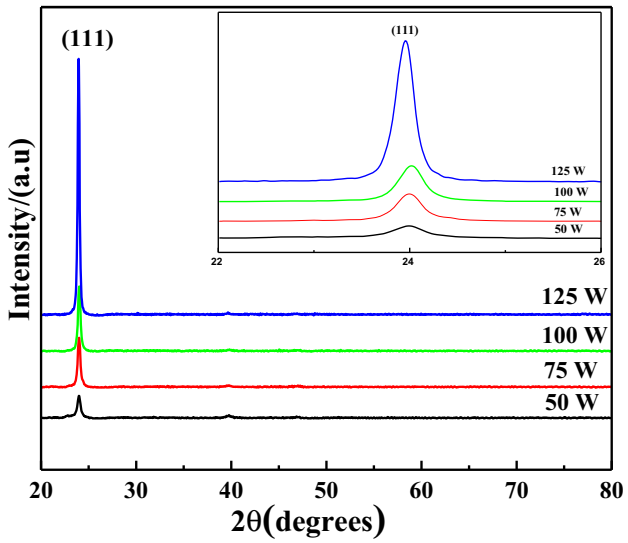

Fig. 1. XRD pattern of $Cd_{1-x}Zn_xTe$ films deposited at different powers.

Table I. Sputtering parameters

Sputtering power (W)	Sputtering pressure (Pa)	Substrate temperature (°C)
50	0.8	Ambient temperature
75		
100		
125		
125	0.3	Ambient temperature
	0.5	
	0.8	
	1.0	
125	0.8	100
		200
		300

Table II. The XRD data of CdZnTe films deposited at various sputtering powers

Power (W)	2θ (°)	Lattice parameter (α) (Å)	d (Å)	FWHM (°)	Grain size (nm)	RMS roughness (nm)
50	23.993	6.4188	3.7059	0.446	17.998	1.85
75	23.993	6.4188	3.7059	0.339	23.722	1.30
100	24.019	6.4118	3.7019	0.326	24.669	1.16
125	23.954	6.4292	3.7119	0.243	33.091	2.54

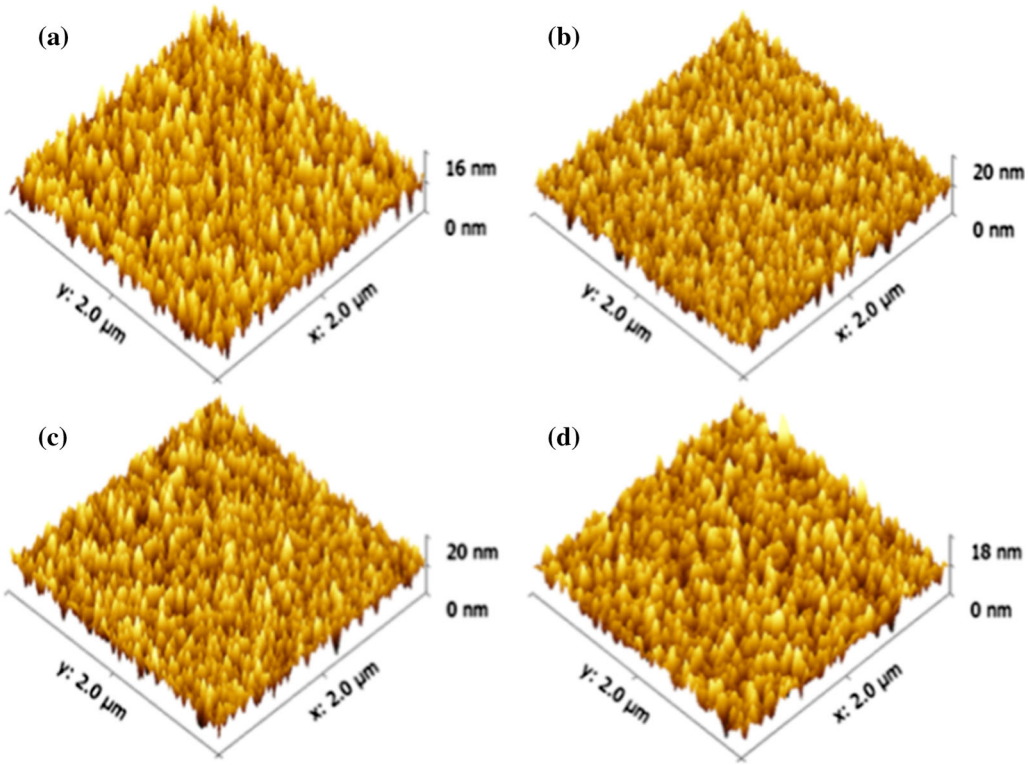

Fig. 2. AFM images of $Cd_{1-x}Zn_xTe$ films deposited at different powers (a) 50 W, (b) 75 W, (c) 100 W, and (d) 125 W.

XRD patterns of the films deposited at different sputtering pressures were shown in Fig. 3. The results show that by increasing the deposition pressure, the intensity of the (111) diffraction peak increases and FWHM of the (111) peak decreases. With the increase of deposition pressure from 0.3 Pa to 1.0 Pa, the (111) diffraction peak gradually shifted to a large angle which may be due to different Zn content (x) in $Cd_{1-x}Zn_xTe$ films.

The Zn content of the films can be calculated by the Vegard's Law.[21]

$$\alpha(Cd_{1-x}Zn_xTe) = (1-x)\cdot\alpha(CdTe) + x\cdot\alpha(ZnTe) \quad (2)$$

where a_{CdTe} = 6.481 Å, a_{ZnTe} = 6.103 Å. The calculated lattice parameter (α) and Zn concentration (x) of the films were listed in Table III. The Zn content of the films increases as the sputtering pressure increases.[15] When the sputtering pressure change from 0.5 Pa to 1.0 Pa, there is no significant change in the FWHM value of the films.

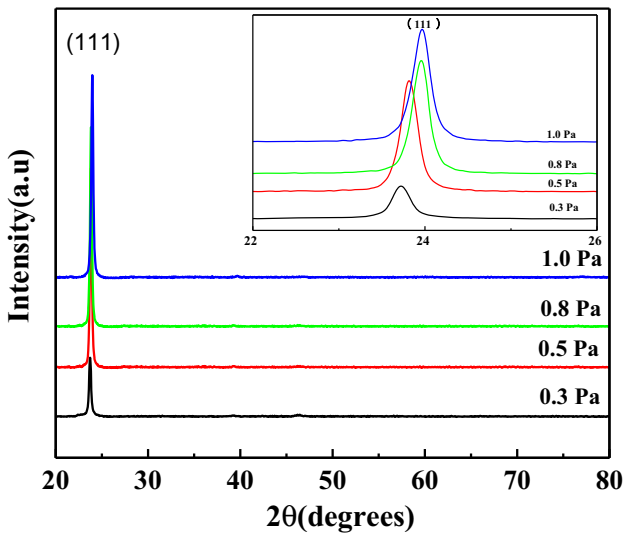

Fig. 3. XRD pattern of $Cd_{1-x}Zn_xTe$ films deposited at different pressures.

Table III. The XRD data of CdZnTe films deposited at various sputtering pressure

Pressure (Pa)	2θ (°)	Lattice parameter (α) (Å)	D (Å)	FWHM (°)	Grain size (nm)	Zn concentration (x)	RMS roughness (nm)
0.3	23.718	6.4922	3.7483	0.288	27.908	–	1.74
0.5	23.830	6.4621	3.7309	0.246	32.680	0.0486	1.78
0.8	23.954	6.4292	3.7119	0.243	33.091	0.1369	2.54
1.0	24.032	6.4080	3.6999	0.245	32.826	0.1929	1.86

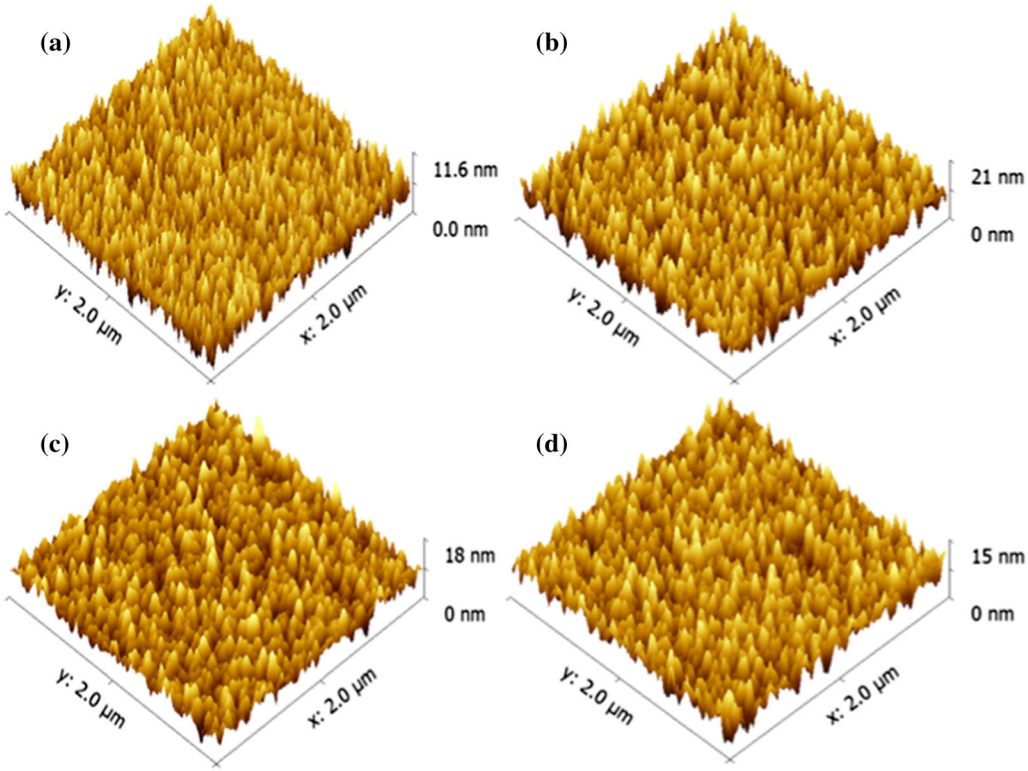

Fig. 4. AFM images of $Cd_{1-x}Zn_xTe$ films deposited at different pressures (a) 0.3 Pa, (b) 0.5 Pa, (c) 0.8 Pa, and (d) 1.0 Pa.

Figure 4 presents AFM images of the films deposited at different pressure. The grain size of the film increases with the increasing of sputtering pressure. This is consistent with the XRD results. All the films are very smooth with a small value of surface roughness.

XRD pattern of the films deposited at different substrate temperatures range from ambient temperature to 300 °C were displayed in Fig. 5. All the films had similar XRD patterns and preferred along (111) peak, only the films deposited at 100 °C with two peaks of (111) and (220). It appears that a better crystallization quality was observed for the films grown at 200 °C with smaller FWHM of (111) peak. The detailed XRD and AFM results of the films deposited at different substrate temperatures were listed in Table IV.

Figure 6 shows AFM images of $Cd_{1-x}Zn_xTe$ films deposited at different temperatures. It is apparent that the films deposited at ambient temperature,

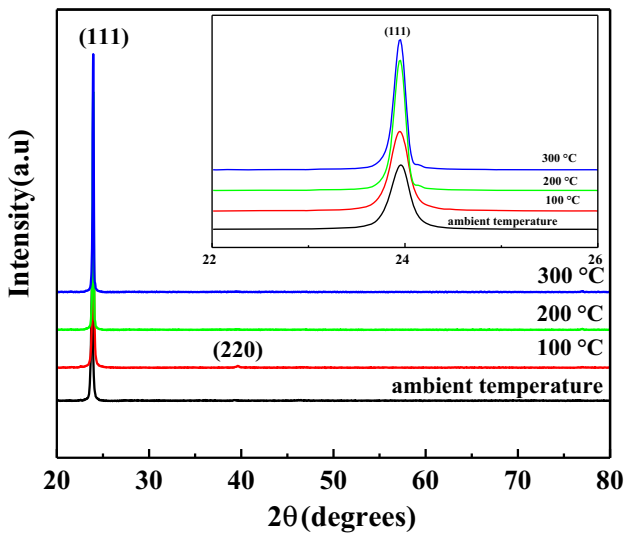

Fig. 5. XRD pattern of $Cd_{1-x}Zn_xTe$ films deposited at different substrate temperatures.

Table IV. The XRD data of CdZnTe films deposited at various substrate temperatures

Temperature (°C)	2θ (°)	Lattice parameter (Å)	d (Å)	FWHM (°)	Grain size of AFM (nm)	RMS roughness (nm)
Ambient temperature	23.954	6.4292	3.7119	0.243	63	2.54
100	23.941	6.4326	3.7139	0.224	70	1.84
200	23.953	6.4294	3.7120	0.148	89	1.51
300	23.928	6.4361	3.7159	0.185	108	2.13

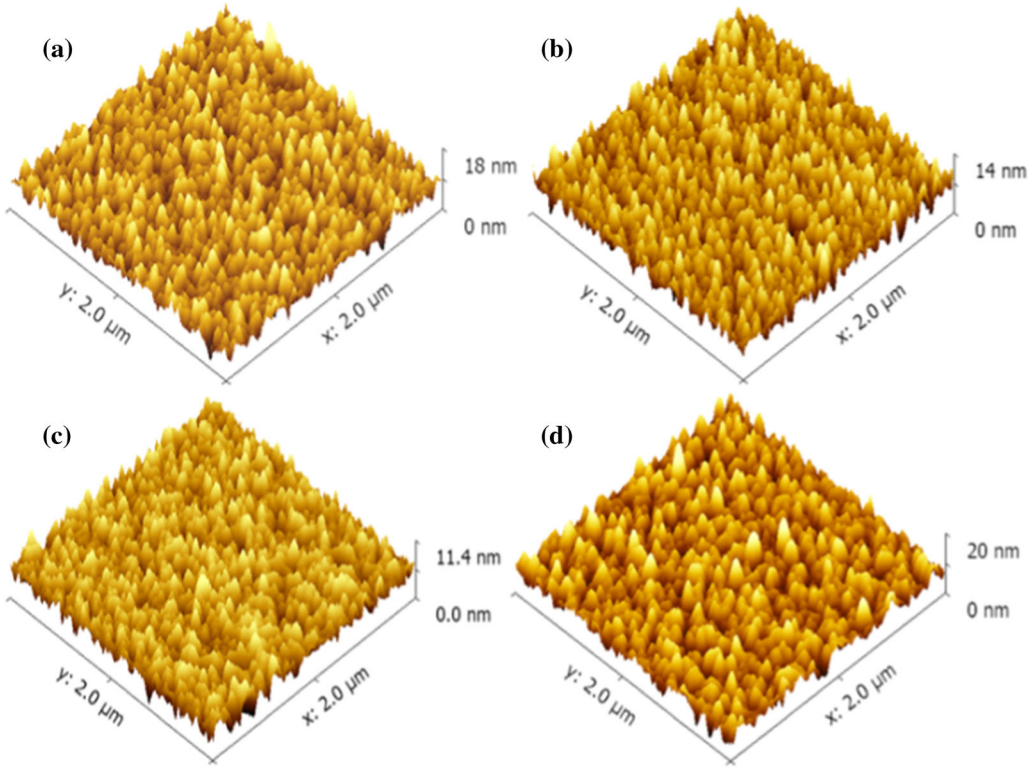

Fig. 6. AFM images of $Cd_{1-x}Zn_xTe$ films deposited at different substrate temperatures (a) ambient temperature, (b) 100 °C, (c) 200 °C, and (d) 300 °C.

100 °C, 200 °C, and 300 °C are spherical in shape with mean diameters of about 63 nm, 70 nm, 89 nm, and 108 nm, respectively. This may in part be due to dynamic factors during sputtering growth.[22] RMS roughness of the films decreases first and then increases as temperature increases as shown in Table IV.

XRD pattern of the films as-grown and annealed at different temperatures are illustrated in Fig. 7. It can be found that the diffraction intensity of the (111) peak of the films is higher than that of the films as-grown after annealing at 200 °C or 300 °C. The appearance of (220), (311), (331), (422) and (511) diffraction peaks after annealing at 400 °C in $CdCl_2$ atmosphere reveals the orientation change and polycrystalline nature of the films.[23–26] In addition, the (111) peak intensity gradually decreases which is related to the occurrence of grain reorientation and recrystallization.[27]

It can be seen that the grain size of the films becomes larger after annealing for grain boundary migration and grain growth from Fig. 8. Furthermore, the grain morphology of the films tends to be more sharp than smooth.

Figure 9 shows that the resistivity of the film decreases with the increase of annealing temperature.[28] After the treatment of $CdCl_2$, the resistivity of the $Cd_{1-x}Zn_xTe$ film decreased, which is similar to the results of CdTe films.[29] The diffusion of chloride ions in films and the change of film properties may be the reasons for the change of resistivity.[29]

CONCLUSIONS

$Cd_{1-x}Zn_xTe$ films were acquired by RF magnetron sputtering on borosilicate glass deposition from the $Cd_{0.8}Zn_{0.2}Te$ target. The influence of sputtering power, sputtering pressure, substrate temperature and annealing on the films properties have been invested. The increases of sputtering power can bring about the grain size of the films to increase, and temperature induces an increase of the grain size. The Zn concentration x of the films increases with the sputtering pressure. Better quality films were achieved for the films deposited at 125 W, 0.8 Pa and 200 °C. The effects of different annealing temperatures in $CdCl_2$ atmosphere on the properties of $Cd_{1-x}Zn_xTe$ were investigated. The resistivity of the films decreases with the increase of annealing temperature in $CdCl_2$ atmosphere.

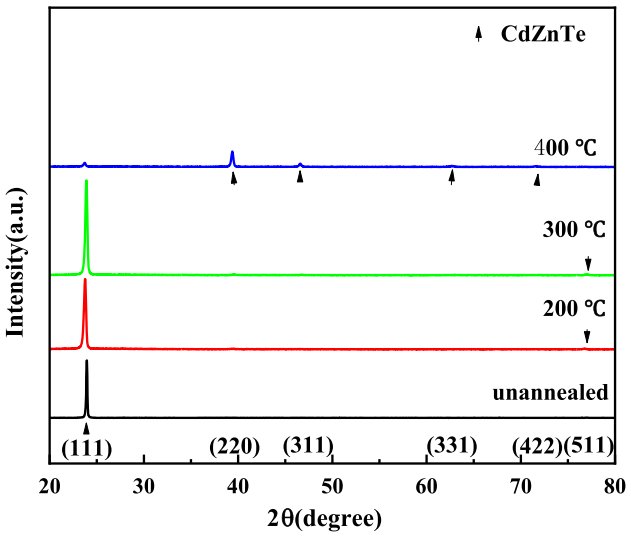

Fig. 7. XRD pattern of as-grown $Cd_{1-x}Zn_xTe$ films and films annealed at different temperatures.

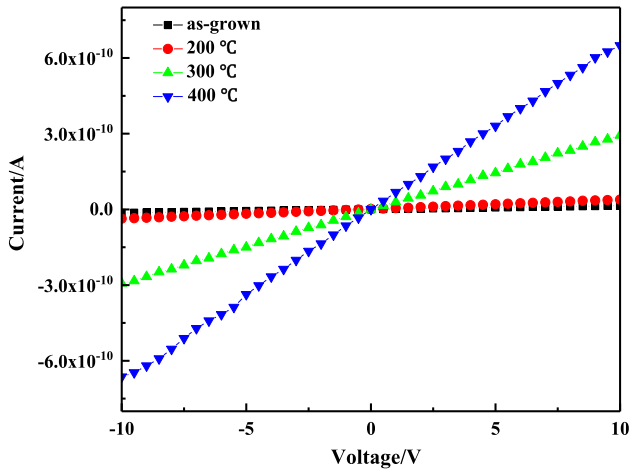

Fig. 9. The *I–V* characteristics of the films as-grown and annealed at different temperatures.

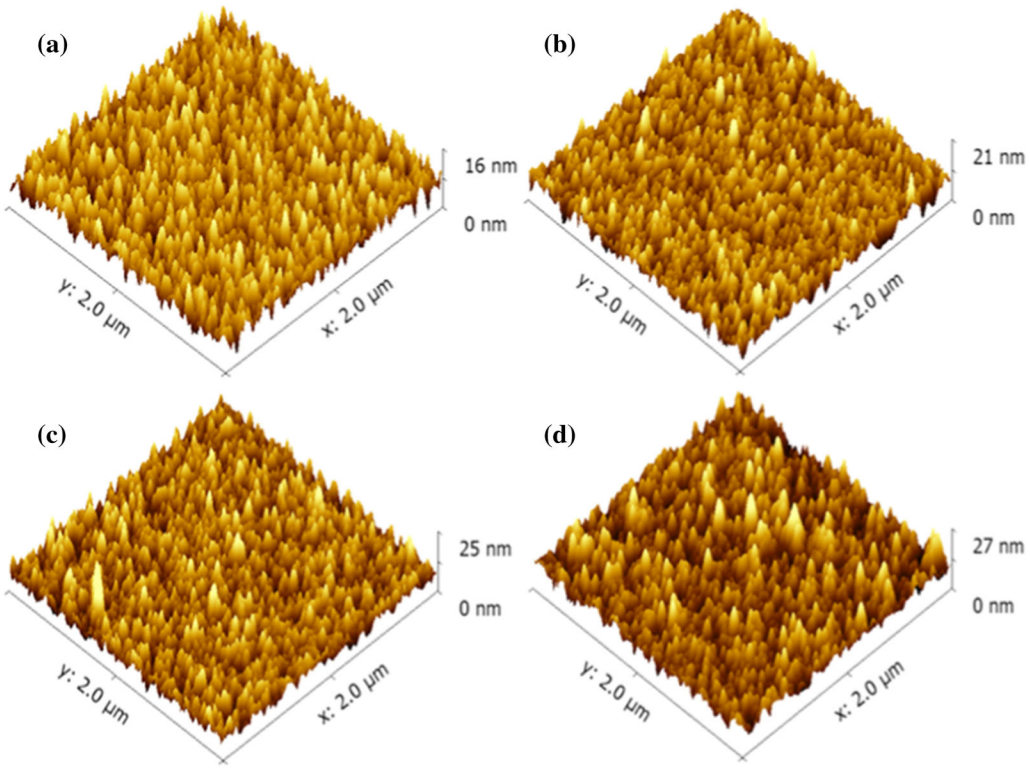

Fig. 8. AFM images of $Cd_{1-x}Zn_xTe$ films annealed at different temperature (a) as-grown, (b) 200 °C, (c) 300 °C, and (d) 400 °C.

ACKNOWLEDGMENT

This work was funded by the National Natural Science Foundation of China (Nos. 11875186, 11905121, and 11775139).

REFERENCES

1. N. Amin, A. Yamada, and M. Konagai, *Jpn. J. Appl. Phys.* 41, 5R (2002).
2. M.J.A. van Pamelen, and C. Budtz-Jorgensen, *J. Nucl. Instrum. Methods Phys. Res.* 411, 197 (1998).
3. M. Singh and E. Mumcuoglu, *IEEE Trans. Nucl. Sci.* 45, 1158 (1998).
4. S. Del Sordo, L. Abbene, E. Caroli, A.M. Mancini, A. Zappettini, and P. Ubertini, *Sensors* 9, 5 (2009).
5. S. Tokuda, H. Kishihara, S. Adachi, and T. Sato, *J. Mater. Sci. Mater. Electron.* 15, 1 (2004).
6. H. Xu, R. Xu, J. Huang, J. Zhang, K. Tang, and L. Wang, *Appl. Surf. Sci.* 305, 477 (2014).
7. A.E. Al-salami, A. Dahshan, and E.R. Shaaban, *Optik* 150, 34 (2017).
8. J. Hu, H. Xiao, G. Liang, Z. Su, P. Fan, and X. Lin, *J. Alloys Compd.* 765, 888 (2018).
9. S.S. Fouad, I.M. El Radaf, P. Sharma, and M.S. El-Bana, *J. Alloys Compd.* 757, 124 (2018).
10. R.K. Savkina, A.B. Smirnov, and F.F. Sizov, *Semicond. Sci. Technol.* 22, 97 (2007).
11. X. Gao, X. Zhu, H. Sun, D. Yang, P. Wangyang, and S. Zhu, *J. Mater. Sci. Mater. Electron.* 28, 5 (2017).
12. Z. Zhu, L. Wu, W. Li, L. Feng, J. Zhang, W. Wang, G. Zeng, and D. Leng, *Vacuum* 103, 43 (2014).
13. H.H. Ji, J. Huang, L. Wang, J.N. Wang, J.M. Lai, R. Xu, J.J. Zhang, Y. Shen, J.H. Min, L.J. Wang, and Y.C. Lu, *Appl. Surf. Sci.* 388, 444 (2016).
14. H. Katagiri, K. Jimbo, W.S. Maw, K. Oishi, M. Yamazaki, H. Araki, and A. Takeuchi, *Thin Solid Films* 517, 7 (2009).
15. A.S. Pugalenthi, R. Balasundaraprabhu, S. Prasanna, K. Thilagavathy, N. Muthukumarasamy, and S. Jayakumar, *Mater. Technol.* 30, 4 (2015).
16. S. Chander and M.S. Dhaka, *Thin Solid Films* 625, 131 (2017).
17. K. Cao, W. Jie, G. Zha, R. Hu, S. Wu, and Y. Wang, *Vacuum* 164, 319 (2019).
18. H. Cao, J.H. Chu, S.L. Wang, Y.H. Wu, and C.J. Zhang, *J. Infrared Millim. Waves* 32(2), 97 (2013).
19. M. Gulen, G. Yildirim, S. Bal, A. Varilci, I. Belenli, and M. Oz, *J. Mater. Sci. Mater. Electron.* 24, 2 (2013).
20. B.D. Cullity, *Elements of X-ray Diffraction*, 3rd edn. (Reading, Addition-Wesley, 2001).
21. E. Yilmaz, E. Tuğay, A. Aktağ, I. Yildiz, M. Parlak, and R. Turan, *J. Alloys Compd.* 545, 90 (2012).
22. D.M. Zeng, W.Q. Jie, H. Zhou, and Y.G. Yang, *Nucl. Instrum. Methods Phys. Res. Sect. A Accel. Spectrom. Detect. Assoc. Equip.* 614, 68 (2010).
23. S.H. Lee, A. Gupta, S. Wang, A.D. Compaan, and B.E. Mccandless, *Sol. Energy Mater. Sol. Cells* 86, 551 (2005).
24. S.N. Vidhya, O.N. Balasundaram, and M. Chandramohan, *Optik* 126, 24 (2015).
25. S. Chander, A.K. De, and M.S. Dhaka, *Sol. Energy* 174, 757 (2018).
26. N. Jia, Y. Xu, R. Guo, Y. Gu, X. Fu, Y. Wang, and W. Jie, *J. Cryst. Growth* 457, 343 (2017).
27. J. Luschitz, K. Lakus-Wollny, A. Klein, and W. Jaegermann, *Thin Solid Films* 515, 15 (2007).
28. M. Emziane, K. Durose, N. Romeo, A. Bosio, and D.P. Halliday, *Thin Solid Films* 480, 377 (2005).
29. S. Babar, P.J. Sellin, J.F. Watts, and M.A. Baker, *Appl. Surf. Sci.* 264, 681 (2013).